Materials Chemistry and Physics 139 (2013) 423–430

Contents lists available at SciVerse ScienceDirect

Materials Chemistry and Physics

journal homepage: www.elsevier.com/locate/matchemphys

Photocatalytic degradation of 2,4-dichlorophenoxyacetic acid under visible light: Effect of synthesis route

K. Del Ángel-Sanchez [a], O. Vázquez-Cuchillo [b,c], A. Aguilar-Elguezabal [a], A. Cruz-López [b,*], A. Herrera-Gómez [d]

[a] Centro de Investigación en Materiales Avanzados (CIMAV), Ave. Miguel de Cervantes 120, Complejo Industrial Chihuahua, 31109 Chihuahua, Chihuahua, Mexico
[b] Universidad Autónoma de Nuevo León, Facultad de Ingeniería Civil, Av. Universidad S/N, Cd. Universitaria, 66451 San Nicolás de los Garza, N. L., Mexico
[c] Universidad Politécnica Metropolitana de Puebla, Circuito de las Flores S/N U. Hab. Mateo de Regil, Puebla, Puebla C.P. 72464, Mexico
[d] Centro de Investigación y de Estudios Avanzados del Instituto Politécnico Nacional, Unidad Querétaro, Libramiento Norponiente #2000, Fracc. Real de Juriquilla, 76230 Querétaro, Querétaro, Mexico

HIGHLIGHTS

- Two routes to incorporate urea as nitrogen precursor at TiO_2 were studied.
- Nitrogen incorporation modifies the band gap energy at TiO_2 structure.
- The doped materials are driven in visible light.
- Sonochemical enhances photodegradation in comparison with sol–gel method.
- 2,4-Dichlorophenoxyacetic is proposed as main degradation reaction.

GRAPHICAL ABSTRACT

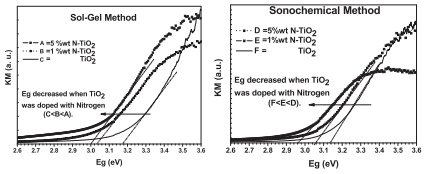

ARTICLE INFO

Article history:
Received 10 July 2012
Received in revised form
4 December 2012
Accepted 5 January 2013

Keywords:
Ceramics
Chemical synthesis
Inorganic compounds
Nanostructures
Semiconductors

ABSTRACT

The photocatalytic degradation of 2,4-dichlorophenoxyacetic acid (2,4-D) under visible light exposure was studied using TiO_2 and TiO_2 doped with nitrogen (1% and 5%) that was prepared by the sol–gel (SG) and sonochemistry (SQ) methods. In fact, the sonochemical route represents a sustainable alternative for saving energy during the synthesis. The results show that the half-life time ($t_{1/2}$) was 71 min for the 5% N–TiO_2 photocatalyst prepared by the SQ. According to XRD results, semi-crystalline TiO_2 was obtained using both synthetic routes at 400 °C. However, the presence of a dopant using the SG method causes an increase in the crystallinity of the TiO_2 materials prepared, and the crystallinity of the SQ route is inhibited at higher nitrogen content. The XPS data showed the presence of nitrogen (398–401 eV) in synthesized TiO_2. The results of the band gap energy (Eg) using a Kubelka–Munk transformation indicate that both methods of synthesis show higher absorbances when nitrogen was incorporated into the matrix of TiO_2, leading to the decrease of Eg from 3.2 eV to 3.0 eV. The TEM analysis shows that the nanoparticles were obtained with sizing less than 40 nm, and the incorporation of nitrogen causes a decrease in the particle size. Finally, the surface properties are consistent with the observed crystallinity in the materials.

1. Introduction

Phenoxyacetic and chlorophenol derivatives are important classes of herbicides that are widely used for weed control in agricultural crops. 2,4-Dichlorophenoxyacetic acid (2,4-D) is one of

* Corresponding author. Tel.: +52 8114424400; fax: +52 8114424443.
E-mail address: cruz_lopeza@yahoo.com.mx (A. Cruz-López).

0254-0584/$ – see front matter © 2013 Elsevier B.V. All rights reserved.
http://dx.doi.org/10.1016/j.matchemphys.2013.01.009

the most commonly used herbicides in Mexico [1] and is the third most widely used herbicide in North America. 2,4-D has been used for agricultural, industrial and urban development, and has been used extensively in agriculture to control broadleaf [1,2]. However, this herbicide is potentially dangerous to animals and humans. For instance, the biodegradability of 2,4-D is extremely low; thus, 2,4-D is a major pollutant in groundwater and surface water effluents. Moreover, water contaminated by pesticides is difficult to treat because conventional processes such as biological degradation, coagulation-flocculation, filtration and oxidation with chlorine cannot remove or completely oxidize pesticides [3,4]. Therefore, alternative remediation treatments for water containing trace amounts of herbicides must be developed. Modern methods for the removal of pollutants include advanced oxidation processes such as photocatalysis. Oxidation processes are based on the production of free radicals (•OH), which initiate a sequence of reactions leading to the partial or total destruction of organic pollutants such as chlorophenols, nitrogen-based pesticides and aromatic compounds [5–7].

Among various semiconducting materials, TiO_2 is commonly used due to its high photocatalytic activity, resistance to photocorrosion, photostability, low cost and non-toxicity. Many attempts to sensitize titanium dioxide to the entire visible spectrum have been made. In addition, TiO_2 has been doped with nonmetallic atoms [8,9]. The enhanced photoactivity of doped TiO_2 has been attributed to an increase in the specific surface area, modifications to the band gap energy, magnification of crystalline defects and morphology, and the modification of the size of titania crystals, which is the predominant crystalline phase of the material. Due to the enhanced photoactivity of the materials, a variety of methods have been developed for the synthesis of semiconductors, including the hydrothermal method [10], the templating method [11], the sol–gel method [12] and the colloidal method [13].

According to the literature, the sol–gel method is relatively simple but is disadvantageous because it lacks precise control of its synthetic parameters, which ultimately leads to poor definition of the mesoporous structure [14]. However, Yamamoto reported that in the process to obtain nanometric particles, the conduction or valence bands can be incremented or diminished, respectively, and he mentioned that variations in the sizes of particles larger than 0.2 nm produce changes of 0.14 eV [15]. On the other side, the novelty of sonochemical method is the source that promotes the chemical reaction; it represents a sustainable alternative for saving energy during the synthesis of nanoparticles [16].

Until now, the effects of the synthesis analysis are not very clear. The electronic modification of titanium oxide through a doping process with rare earth [17], metallic elements [18], or nonmetallic elements [19,20], has garnered excellent results in different applications. TiO_2 that is doped with nitrogen has had promising results as a photocatalyst in the visible region. Different routes have been reported for the doping of P25 with nitrogen, including a thermal treatment of NH_3 gas [21,22], the oxidation of TiN [23], the treatment of TiO_2 with a mixture of urea [24–26] and in the screening of TiO_2 via sputtering in a N_2 atmosphere [27].

Through the combination of optical and electronic factors, explanations have been given for the improvement of the catalytic activity of the N–TiO_2 under the absorption of visible light. However, until now, a comparative study of the physicochemical properties of TiO_2 that has been doped with 1 and 5% of nitrogen using routes of synthesis (sol–gel and sonochemistry methods) has not been reported; the objective of this study is to determine the influence of the preparation method on the photocatalytic properties for the degradation of 2,4-dichlorophenoxyacetic acid under visible light exposure.

2. Experimental part

2.1. Sol–gel method

The synthesis of TiO_2 by the sol–gel method at room temperature was carried out using titanium (IV) butoxide (97% reactive grade; Sigma Aldrich), deionized water and concentrated nitric acid (DEQ). A 3-neck flask, was used over a heater and filled with an inert atmosphere. Then, an acidic aqueous solution was added (molar ratio water/acid = 420), and the mixture was subjected to vigorous mechanical stirring. A volume of titanium butoxide, corresponding to the molar ratio of water/alkoxide = 43 and acid/alkoxide = 0.14, was then added. After the addition of the alkoxide for 2 h, the reaction was stopped using the procedure described above [18].

The solids obtained were dried in an oven at 100 °C for 24 h and were annealed at 400 °C for 4 h using a heating ramp of 1 °C min^{-1} to obtain a crystalline material with some signs of carbon residues (yellow color).

2.2. Sonochemical method

For this method, the same titanium butoxide was used, but the reactive medium was a mixture of 50% acetone (99.5% DEQ) and 50% methanol (99.5% DEQ) to prevent the hydrolysis of the titanium butoxide. A 3-necked flask was immersed into an ultrasound bath (Branson) in a controlled atmosphere [28]. Then, a bypass valve was opened, and the 1:1 acetone–ethanol mixture by volume was added. To this mixture, the titanium butoxide was slowly added in a molar acid/alkoxide ratio = 0.14, and the reaction was initiated through low intensity radiation for 1 h. A system with recirculating cooling water was used to secure ambient temperature for the reaction.

A milky white solution was obtained when the reaction was complete, and it was dried in the oven at 100 °C for 24 h. Finally, this material was calcined at 400 °C for 4 h with a heating ramp of 1 °C min^{-1}.

2.3. TiO_2 doped with nitrogen

For each of the synthetic routes described above, the titanium oxide samples were doped with 1% and 5% of nitrogen. For each of the preparation methods, urea was used as the nitrogen precursor. In each case, the urea was diluted in an aqueous solution in the flask with vigorous stirring, and the reactants were added. The reaction mixture was stopped after stirring for 2 h [18,28], and the samples were treated with the thermal treatments described above.

2.4. Characterization

To determine phases that were present in the TiO_2 samples, the D8 advance X-ray diffraction equipment was used. The analyses of the photoelectronic spectroscopy that was issued by the X-rays were used to determine the composition and the electronic structure of the doped samples using an Intecovamex Equipment XPS 110. The morphology and the size of the particles were determined using a JEOL-649LV electron scanning microscope, and the particles were staged in an EDE detector INCA-Xsight. The N_2-physisorption on the surface and the texture of the samples of the prepared TiO_2 were evaluated using an analyzer Quantacrome Instrument Nova 2000e. The energy gap (Eg) was determined through the diffuse reflectance spectra of a UV–Vis Perkin–Elmer Lambda 35 using the Kubelka–Munk theory.

2.5. Photocatalytic activity

The photodegradation of 2,4-dichlorophenoxyacetic acid (2,4-D) using visible light was studied using titanium oxides and the titanium oxides doped with nitrogen. According to the experimental procedure, a lamp with the following characteristics [GaI3 250 W (400–700)] was placed inside of the reactor, which contains 100 mg of the catalyst and 100 mL of the aqueous solution with an initial concentration of 40 ppm (1.8E-04 M). Both of the materials were mixed using mechanical stirring for 30 min with the passage of a flux of air (5 mL min^{-1}) to study the saturation of oxygen in the samples. Before the study, the mechanical agitation continued in the absence of light for 1 h to achieve an adsorption–desorption equilibrium between the surface of the photocatalyst and the pollutant. Next, the solution was irradiated with light for 2 h. During this time, 1 mL aliquots of the solution were taken at regular intervals, and these samples were analyzed by UV–Vis spectroscopy to calculate the photodegradation. The photodegradation was monitored through the main adsorption band at 229 nm versus the time of irradiation using the Perkin Elmer Landa25 UV–Vis spectrophotometer. The mineralization was measured by total organic carbon (TOC) on a Shimadzu VCSN TOC analyzer. Those analyses were performed before and after the photodegradation.

3. Results and discussion

3.1. X-ray diffraction

Fig. 1 shows the results of the X-ray diffraction analysis of the TiO_2 that was prepared by different synthetic routes and calcinated at 400 °C for 4 h. According to the images, the crystals obtained had anatase reflections with characteristics close to the following angles: $2\theta = 25.3, 37.0, 37.8, 38.6, 48.1, 53.9, 55.1, 62.2, 62.8, 68.8$, and the corresponding Miller indexes are (*101*), (*103*), (*004*), (*112*), (*200*), (*105*), (*211*), (*213*), (*204*) and (*116*), respectively, according to the JCPS-card 894921. These results are in accordance with previous studies that have been reported [13].

Although the materials were prepared using the same stoichiometric ratios, the degree of crystallinity of the titanium oxides differed significantly. This observation suggests that there is an implicit effect on the synthesis methodology. In the sol–gel route [29], the behavior is not easily predictable; however, the synthetic conditions, including the presence of a hydrolysis catalyst that is selective to attack the O–R bond (where R = CH_3–CH_2–CH_2–CH_2) in titanium butoxide structure causing the rapid formation of $Ti(OH)_4$ and it favors an orderly arrangement of the structure and forms a semi-crystalline material after the calcinations [23].

In contrast, in the case of the TiO_2 that was prepared by the sonochemical route, the impact of the acoustic cavitations (42 kHz) of traveling through liquids causes that the bonds of the alkoxide in the solution might breakdown slowly; This improvement is probably the result of a very slow breakdown of the alkoxide chains because the ultrasound waves allow a slower nucleation and a more orderly arrangement; thus, increasing the crystallinity of the prepared samples promote the fast recombination rate between Ti–O to generate a higher degree of order in the structure. This result is in accordance with the results published by other authors who improved the crystallinity of TiO_2 using ultrasound waves [30,31].

Fig. 2-I presents the reflections of titanium oxide doped with nitrogen (1% and 5% N) prepared by the sol–gel method. For this series of experiments, we observed a significant increase in the intensity of the peaks as the amount of nitrogen added is increased. This trend, maybe explained that during the hydrolysis step because the concentration of protons from urea is high, then the Ti–OH is protonized to generate $Ti(OH)_2^+$, and so $[TiO_6]$ octahedral prefer to attach to the protons, forming $[TiO_6]^{n+}$ network [32]. The results are consistent with reports from S. Livraghi [30], who reported that the kinetics of the reaction is favored by the presence

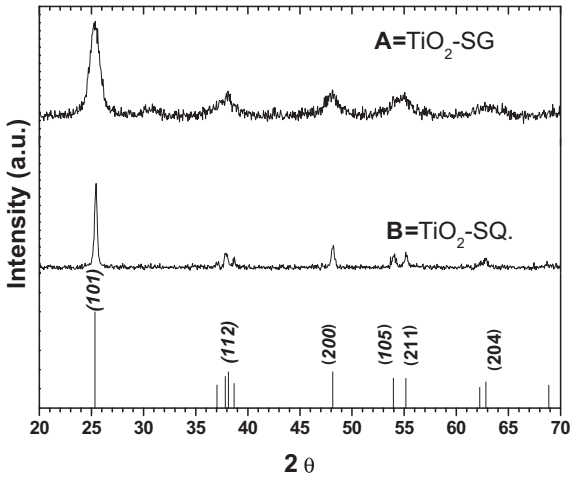

Fig. 1. X-ray diffraction of TiO_2 prepared by different routes of synthesis and calcined at 400 °C. A) TiO_2-SG, B) TiO_2-SQ.

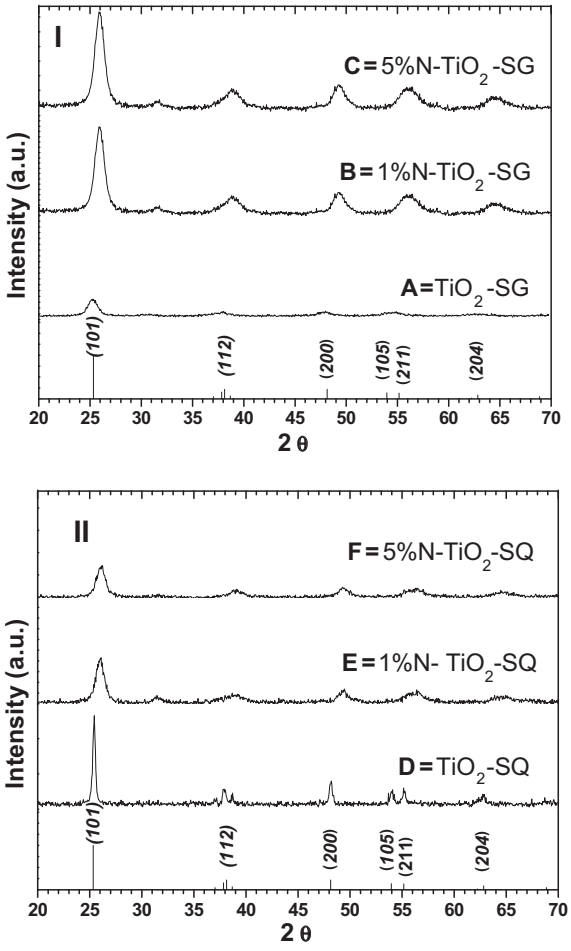

Fig. 2. X-ray diffraction of TiO_2 and TiO_2 doped with different concentrations of nitrogen and calcined at 400 °C. I) Sol–Gel (SG), II) Sonochemistry (SQ).

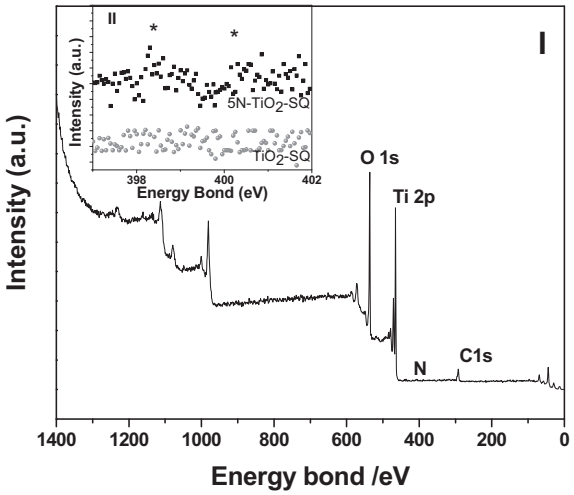

Fig. 3. X-photoelectron analysis of the sample, 5% N–TiO_2-SQ calcined at 400 °C. I) Record of the sample in the range from 0 to 1400 eV. II) Comparative N 1 s record of doped sample compared with TiO_2 in the range 398–402 eV (inset).

of complex nitrogen which slows the kinetics by changing the reaction pH to 9 and results in an increase of crystallinity that increases the amount of the urea precursor in the sample. By this synthesis route, it is well known that if during the preparation of TiO_2 the sol has an alkaline pH, the crystallinity and the particle size are strongly modified to obtain nanoparticles [32–35].

Fig. 2-II shows the diffractograms of the samples doped with titanium oxide and nitrogen obtained by the sonochemical route. For this series of materials, the presence of the dopant caused a light displacement of the main reflections of TiO_2 but the main characteristic is a diminishing in the intensity of the reflections with respect to the undoped TiO_2. One possible explanation for this behavior could be attributed to the cavitation process that causes the breaking of chains in the nitrogen precursor. It means that N and C act as structural impurities that inhibit the crystallization of N–TiO_2.

3.2. X-ray photoelectron spectroscopy

XPS analyses were performed on the TiO_2 and TiO_2 doped with 5% nitrogen. Fig. 3 shows the results of samples prepared by the sonochemical route. According to the analysis in the range from 0 to 1400 eV, the Ti and O clearly co-exist on the substrate. Furthermore, the insert images graph shows the N 1 s record of samples of 5% N–TiO_2 to 398 eV in comparison with undoped material, probably the signal is weak because the nitrogen is not homogenously dispersed according to the literature, this signal is attributed to nitrogen doping that is interstitially placed in the structure of TiO_2 [31,35–37]. This observation coincides with reports in Ti–O–N [36].

3.3. Transmission electron microscopy

Fig. 4a shows the transmission electron microscopy images of the TiO_2 prepared by sol–gel method. This technique confirmed the ability to obtain nano-sized TiO_2 particles nevertheless the range is wide (from 50 to 30 nm) as showed in Fig. 4b. Moreover, when the nitrogen concentration increased from 1% to 5%, a decrease in particle size from 20 to 10 nm was observed, regardless of the synthetic route used (see Figs. 5 and 6). Similar behavior has been obtained by other authors and shows a decrease in particle size due to the nitrogen precursor during synthesis [38].

3.4. Energy band gap

The samples of TiO_2 and nitrogen-doped TiO_2 prepared by the two synthetic routes were measured by the bandwidth of the reflectance technique and then were adjusted using a Kubelka–Munk transformation, which was reported in a previous work [13].

Fig. 7-I shows the results of samples that were prepared using the sol–gel route and shows that the absorbance increased as a greater amount of synthesized N is incorporated. This finding has been reported for similar nitrogen-doped TiO_2 systems [38] and other systems [39]. In addition, the Eg value is 3.2 eV for the undoped TiO_2 and 3.0 eV for the material with 5% nitrogen. R. Kun in a previous study has reported the relationship between the increase in the absorbance by the presence of N in the material and the observed higher photocatalytic activity of the material [24].

In Fig. 7-II, we present the results of the samples that were prepared by the sonochemical route. In this experiment, we observe a similar behavior, and the sample doped with 5% nitrogen has a bandwidth of 2.95 eV. Table 1 summarizes the Eg values for all samples.

Senthilnathan reported that the shift of the Eg value in the doped samples can be explained by the nature of the nitrogen from organic complexes [39] and that the result is not similar when using ammonia [35,37]. In a previous study it was showed that the decrease of the width of band gap of TiO_2 is attributed to the inclusion of nitrogen and the presence of oxygen defects in the structure [37]. This author declared that the substituted nitrogen atom acts as an acceptor side of the valence band (VB), while the donors are the oxygen defects that disrupt the conduction band (CB).

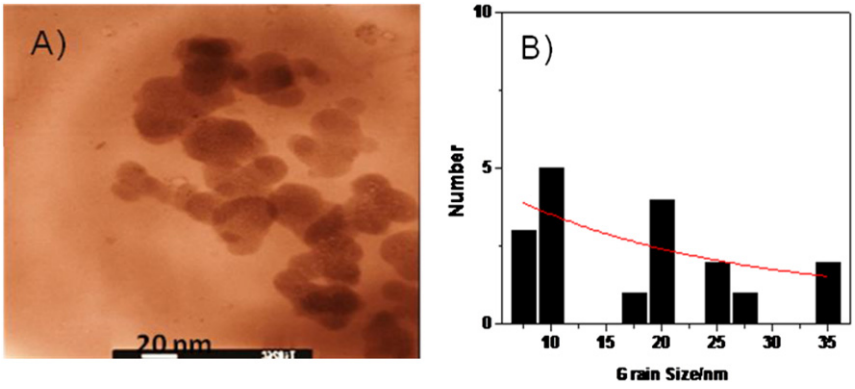

Fig. 4. Transmission electron microscopy of TiO_2 prepared by sol–gel method and calcined at 400 °C. A) Image a 20 nm. B) Size distribution.

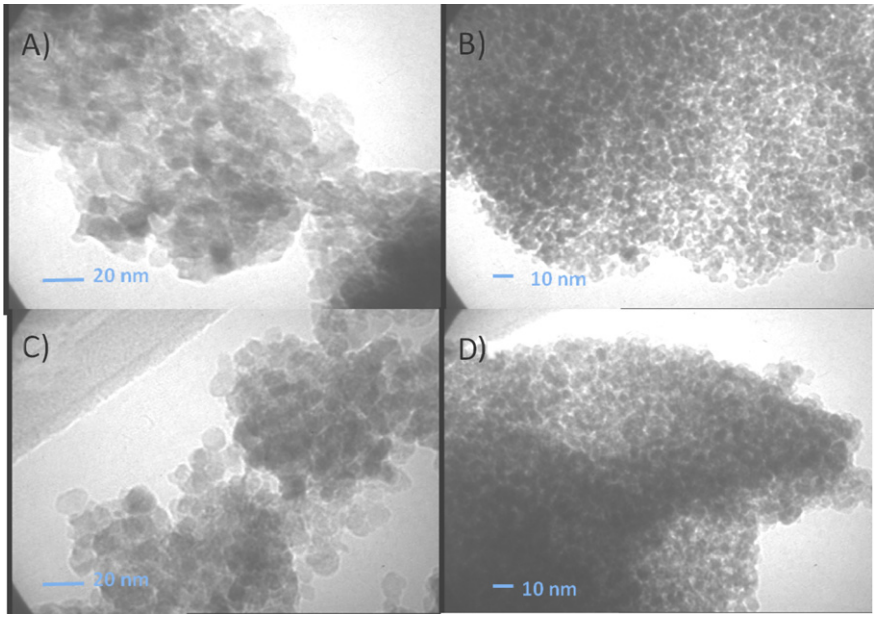

Fig. 5. Transmission electron microscopy of the samples TiO_2 doped with nitrogen prepared by sol–gel method and sonochemical methods and calcined at 400 °C. A) 1%N–TiO_2-SG, B) 5%N–TiO_2-SG, C) 1%N–TiO_2-SQ y D) 5%N–TiO_2-SQ.

3.5. Surface area

To understand the surface properties of materials prepared by soft chemical routes, we proceeded to measure the surface area of TiO_2 and nitrogen-doped TiO_2 that were thermally treated at 400 °C for 4 h (see Table 1). In the case of TiO_2 that was obtained by the sol–gel method, the N_2-physisorption analyses yielded a value of 157 m^2 g^{-1}, and the surface area of the TiO_2 obtained by the

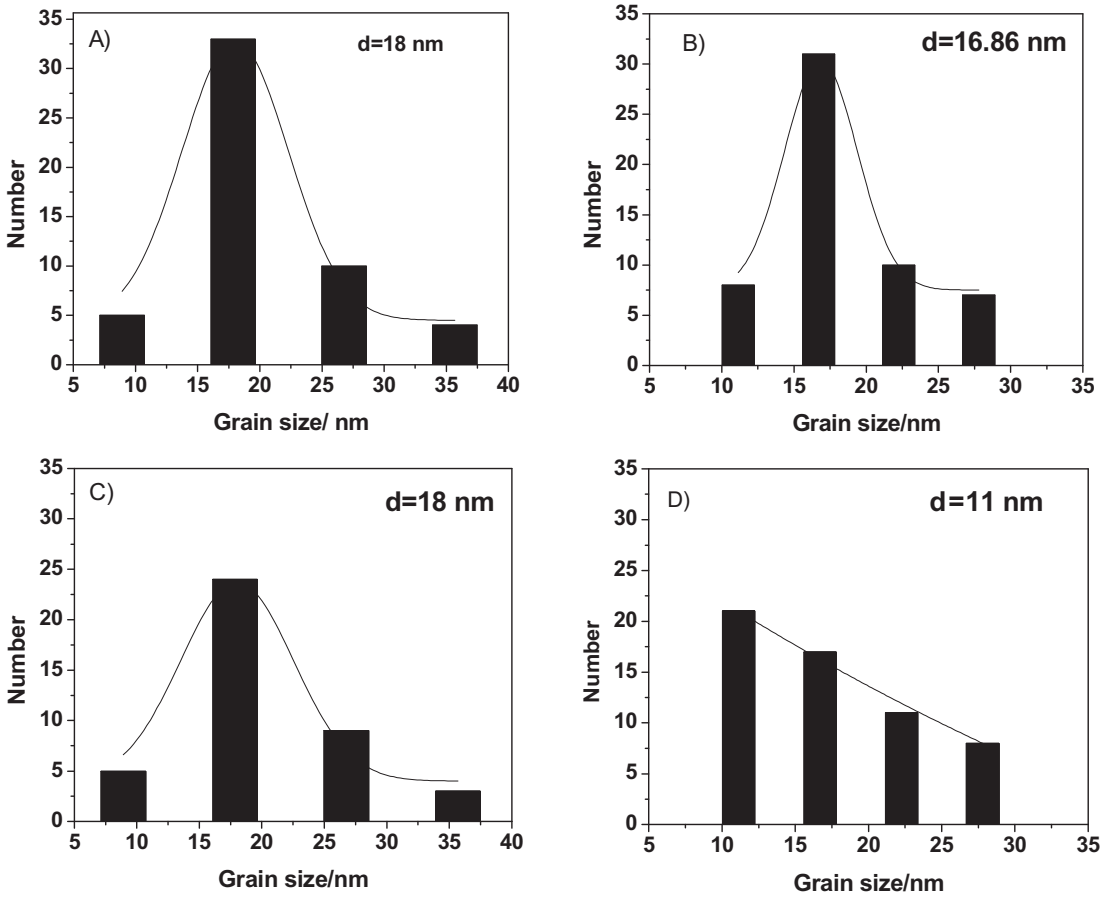

Fig. 6. Particle size distribution histograms for the TiO_2 doped particles prepared by sol–gel method and sonochemical method at 400 °C. A) 1%N–TiO_2-SG, B) 5%N–TiO_2-SG, C) 1% N–TiO_2-SQ y D) 5%N–TiO_2-SQ.

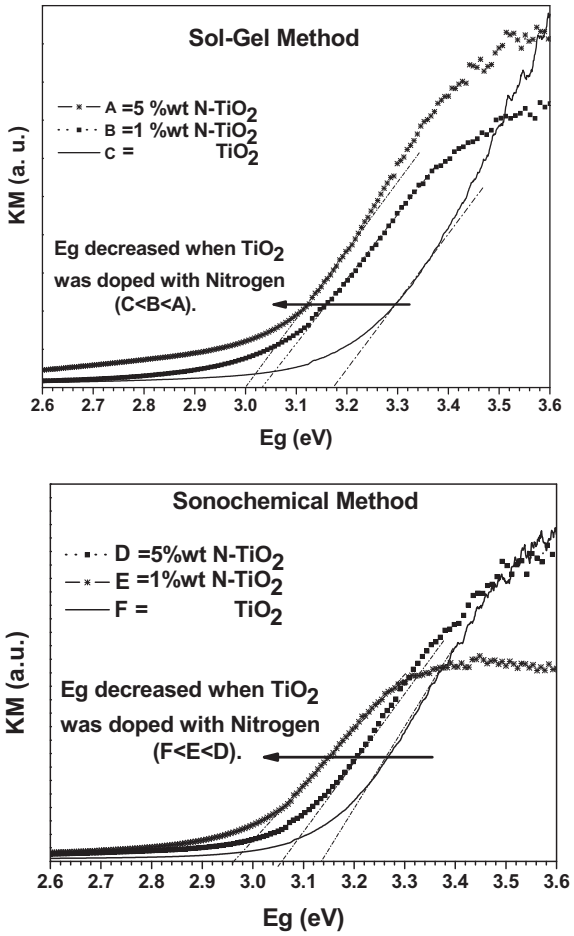

Fig. 7. Energy band gap of nitrogen-doped photocatalysts prepared by the sol–gel and sonochemistry routes.

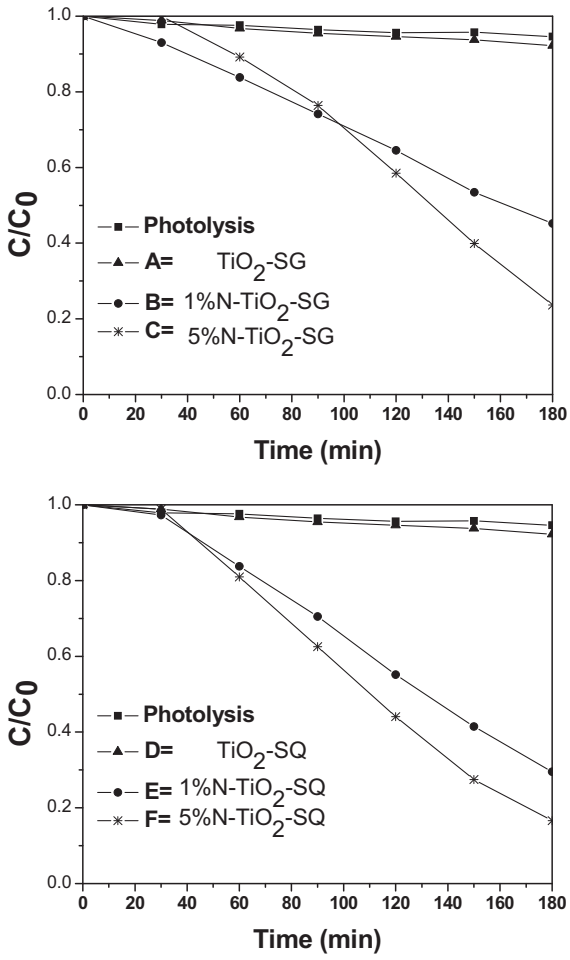

Fig. 8. Photocatalytic activity of TiO_2 and N–TiO_2 materials prepared by different synthesis routes and calcined at 400 °C.

sonochemical route showed a value of 37 $m^2\ g^{-1}$. These results highlighted a marked difference with respect to the synthetic route used as has been seen in XRD. In the materials doped with 1% and 5% nitrogen, the sol–gel route had a 20–30% decrease in surface area; this decrease can be attributed to the change in the rate of hydrolysis due to the pH change by the incorporation of precursors for the synthesis. The nitrogen-doped titanium oxides that were prepared by the sonochemical route presented an opposite trend because the presence of nitrogen produces an increased surface area, and this behavior is due to the nucleation rate as discussed in the XRD section above.

3.6. Photocatalytic degradation of 2,4-D

Fig. 8 shows the degradation of 2,4-D as a function of time, using both the doped and the undoped titanium oxide samples. The corresponding photocatalytic activity is reported as half-life ($t_{1/2}$) in Table 1. In photolytic process, there is a decrease in the activity of only 5% after 180 min of exposure to visible light. Similar trend has been observed for the photocatalytic test using TiO_2 synthesized by sonochemistry method, while the TiO_2 obtained by the sol–gel method was active before 120 min. This effect may be due to the difference in area existing in the two routes of synthesis (sol–gel = 157 $m^2\ g^{-1}$, sonochemistry = 37 $m^2\ g^{-1}$) and the similar Eg values (sol–gel = 3.18 eV, and sonochemistry = 3.15 eV). When N was incorporated into the TiO_2, a radical improvement in the activity was observed. For the 1% N–TiO_2 sample that was synthesized by the sol–gel method, the degradation value was 55% with a $t_{1/2}$ = 224 min. The material synthesized by the sonochemical method had degradation values greater than 71% and $t_{1/2}$ = 100 min. This increased activity was heightened as more nitrogen was incorporated into the material, and degradation values of 76% and 83% were obtained for the 5% N–TiO_2 materials

Table 1
Surface area, band gap energy, kinetic constants and TOC analyses from TiO_2 and N–TiO_2 prepared by two routes of synthesis and calcinated at 400 °C/4 h.

Sample	Synthesis method									
	Sol–gel					Sonochemical				
	AS ($m^2\ g^{-1}$)	Eg (Ev)	k (min^{-1})	t (min)	TOC %	AS ($m^2\ g^{-1}$)	Eg (Ev)	k (min^{-1})	t (min)	TOC %
TiO_2	157	3.18	0.0012	557	–	37	3.15	0.0004	1732	–
1%N–TiO_2	83	3.02	0.0031	224	5	148	3.10	0.0069	100	23
5%N–TiO_2	120	3.00	0.0074	97	30	111	2.95	0.0098	71	44

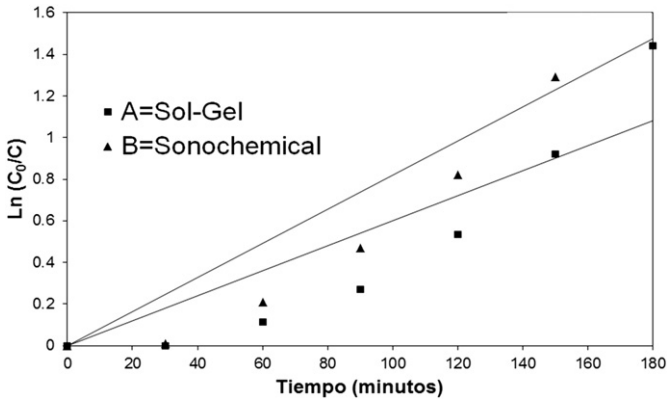

Fig. 9. Graphics of the kinetic model of pseudo-first order of 5%N TiO_2 synthesized by soft chemistry routes. A) Sol-gel and B) sonochemistry.

synthesized by the sol–gel and sonochemical methods, respectively. These samples had half-lives of 97 and 71 min, respectively.

The total organic carbon remaining was measured before for each photocatalytic test (at 3 h) as showed in Table 1. In general there is a huge difference between the TOC abatement efficiencies obtained in the photodegradation of the 2,4-D among the different catalysts. It is worth to mention that most important improvement (44%) was observed with 5% N–TiO_2 materials synthesized by the sonochemical method. For 5%N–TiO_2-SG, 1%N–TiO_2-SQ and 1% N–TiO_2-SG, the TOC removal of the reactant was 30, 23 and 5% respectively.

When the photocatalyst surface is irradiated with visible light, excited electrons are transferred from the valence band to the conduction band, which results in the production of positive holes. The actions of electrons and holes on the substances around them then produce reactive species such as hydroxyl and superoxide radicals. In particular, the hydroxyl radical is required to completely decompose organic compounds. This is probably influenced by the presence of nitrogen interstitially in the structure of TiO_2 was the main reason for the modification of the optical properties of TiO_2 (Eg $<$ 3.0 eV) that make it active in the visible region Therefore, when comparing the results, the synthetic route plays an important role in the rate of the electron–hole recombination, which helps to increase the activity of the material in the 2,4-D degradation under visible light exposure.

This work confirmed that the samples corresponded to a pseudo-first order using the following kinetic model, $C = \mathrm{Co}\cdot e^{-kt}$ (see Fig. 9).

4. Conclusions

This study concluded that it is possible to activate TiO_2 with nitrogen following visible light exposure, using synthetic routes that are less sharp than the traditional thermal treatment with NH_3. For N–TiO_2, we observed a strong effect on the incorporation of nitrogen during synthesis and the physicochemical and photocatalytic properties.

The addition of urea during the synthesis of TiO_2 modifies the mechanism of nucleation as results of change of pH, which causes an outstanding modification of structural, morphological and optical properties.

The photocatalytical degradation of 2,4-dichlorophenoxyacetic acid (2,4-D) under visible light exposure is drastically modified by the incorporation of N in the TiO_2 and decreases the rate of recombination of the electron–hole pairs and increases the degradation of 2,4-D. The herbicide was removed with the materials synthesized by sol–gel as well as with the materials synthesized by sonochemical route.

The sonochemical route represents an alternative for saving energy in a sustainable way in the synthesis of materials. The results show that the half-life time ($t_{1/2}$) was 71 min for the 5% N–TiO_2 photocatalyst prepared by the SQ.

According to the physicochemical characterization, it is concluded that the incorporation of nitrogen into the TiO_2 structure is interstitial. Specifically, the main peak of anatase (101) in XRD did not differ significantly, showing the replacement of nitrogen with titanium. Instead, the band gap energy shows a shift toward the visible region (Eg $<$ 3.2 eV).

Acknowledgments

We are thankful to Luis de la Torre from CIMAV for performing the analyses described in this work. This work was funded by CONACyT (81437). K Ángel-Sanchez wishes to thank to CONACYT for his PhD grant.

References

[1] CICOPLAFEST, Commission for the Process Control and Use of Pesticides and Toxic Substances: Official Catalogue of Pesticides. México, 2004.
[2] PANNA, Pesticide Action Network North America, Pesticides Database – Chemicals (2010).www.pesticideinfo.org.
[3] E. Brillas, J.C. Calpe, P.L. Cabot, Degradation of the herbicide 2,4-dichlorophenoxyacetic acid by ozonation catalyzed with Fe^{2+} and UVA light, Appl. Catal. B 46 (1986) 381–391.
[4] D.G. Hoover, G.E. Borgonovi, S.H. Jones, M. Alexander, Anomalies in Mineralization of low concentrations of organic compounds in lake water and sewage, Appl. Environ. Microbiol. 51 (1986) 226–232.
[5] C. Berberidou, I. Poulios, N.P. Xekoukoulotakis, D. Mantzavinos, Sonolytic, photocatalytic and sonophotocatalytic degradation of malachite green in aqueous solutions, Appl. Catal. B 74 (2007) 63–73.
[6] Z. Baoxiu, Z. Pengyi, Photocatalytic decomposition of perfluorooctanoic acid with β-Ga_2O_3 wide bandgap photocatalyst, Catal. Commun. 10 (2009) 1184–1187.
[7] O. Vázquez-Cuchillo, A. Cruz-López, L.M. Bautista-Carrillo, A. Bautista-Hernández, L.M. Torres Martínez, S. Wohn Lee, Synthesis of TiO_2 using different hydrolysis catalysts and doped with Zn for efficient degradation of aqueous phase pollutants under UV Light, Res. Chem. Intermed. 36 (2010) 103–113.
[8] B. Tian, C. Li, F. Gu, H. Jiang, Synergetic effects of nitrogen doping and Au loading on enhancing the visible-light photocatalytic activity of nano-TiO_2, Catal. Commun. 10 (2009) 925–929.
[9] L. Jia, J. Li, W. Fang, Enhanced visible-light active C and Fe co-doped $LaCoO_3$ for reduction of carbon dioxide, Catal. Commun. 11 (2009) 87–90.
[10] M.M. Titirici, M. Antonietti, A. Thomas, A generalized synthesis of metal oxide hollow spheres using a hydrothermal approach, Chem. Mater. 18 (2006) 3808–3812.
[11] H.S. Qian, G.F. Lin, Y.X. Zhang, P. Gunawan, R. Xu, A new approach to synthesize uniform metal oxide hollow nanospheres via controlled precipitation, Nanotechnology 18 (2007) 355602–355607.
[12] Y.X. Zhang, G.H. Li, Y.C. Wu, T. Xie, Sol–gel synthesis of titania hollow spheres, Mater. Res. Bull. 40 (2005) 1993–1999.
[13] K. Del Ángel-Sanchez, O. Vázquez-Cuchillo, M. Salazar-Villanueva, J.F. Sánchez-Ramirez, A. Cruz-Lopez, A. Aguilar-Elguezabal, Preparation, characterization and photocatalitic properties of TiO_2 nanostructured spheres synthesized by sol–gel method modified with ethylene glycol, J. Sol-Gel Sci. Technol. 58 (2011) 360–365.
[14] M. Alam Khan, M. Shaheer Akhtar, Y. O-Bong, Synthesis, characterization and application of sol–gel derived mesoporous TiO_2 nanoparticles for dye-sensitized solar cells, Solar Energy 84 (12) (2010) 2195–2201.
[15] C. Capiglia, J. Yang, N. Imanishi, A. Hirano, Y. Takeda, O. Yamamoto, Composite polymer electrolyte: the role of filler grain size, Solid State Ionics 154–155 (2002) 7–14.
[16] T.J. Mason, J.P. Lorimer, Applied Sonochemistry the Uses of Power Ultrasound in Chemistry and Processing, Wiley-VCH, 2002, pp. 25–153.
[17] M.A. Rauf, M.A. Meetani, S. Hisaindee, An overview on the photocatalytic degradation of azo dyes in the presence of TiO_2 doped with selective transition metals, Desalination 276 (1–3) (2011) 13–27.
[18] O. Carp, C.L. Huisman, A. Reller, Photoinduced reactivity of titanium dioxide, Prog. Solid State Chem. 32 (1–2) (2004) 33–177.
[19] K.M. Parida, B. Naik, Synthesis of mesoporous TiO_{2-x}–N_x spheres by template free homogeneous co-precipitation method and their photo-catalytic activity under visible light illumination, J. Colloid Interface. Sci. 333 (2009) 269–276.
[20] H. Irie, Y. Watanabe, K. Hashimoto, Nitrogen-concentration dependence on photocatalytic activity of TiO_{2-x}–N_x powders, J. Phys. Chem. B 107 (2003) 5483–5486.

[21] F. Dong, W. Zhao, Z. Wu, S. Guo, Band structure and visible light photocatalytic activity of multi-type nitrogen doped TiO_2 nanoparticles prepared by thermal decomposition, J. Hazard. Mater. 162 (2009) 763–770.
[22] R. Silveyra, L. de la Torres-Sáenz, W. Antunez-Flores, V. Collins Martínez, A. Aguilar Elguezabal, Dopage de TiO_2 con nitrógeno para modificar el intervalo de activación fotocatalítica hacia radiación visible, XIX SICAT 37, September 5–11 (2004) 883792.
[23] F. Xiaoming, Z. Zhengguo, C. Qinglin, J. Hongbing, G. Xuenong, Dependence of nitrogen doping on TiO_2 precursor annealed under NH_3 flow, J. Solid State Chem. 180 (2007) 1325–1332.
[24] R. Kun, S. Tarján, A. Oszkó, T. seemann, V. Zöllmer, M. Busse, I. Dékány, Preparation and characterization of mesoporous N-doped and sulfuric acid treated anatsae TiO2 catalysis and their photocatalytic activity under UV and vis illumination, J. Solid State Chem. 182 (2009) 3076–3084.
[25] K.A. Michalow, D. Logvinovich, A. Weidenkaff, M. Amberg, G. Fortunato, A. Heel, T. Graule, M. Rekas, Synthesis, characterization and electronic structure of nitrogen-doped TiO_2 nanopowder, Catal. Today 144 (2009) 7–12.
[26] C. Belver, R. Bellod, S.J. Stewart, F.G. Requejo, M. Fernández-García, Nitrogen-containing TiO_2 photocatalysts part 2. Photocatalytic behavior under sunlight excitation, Appl. Catal. B 65 (2006) 309–314.
[27] R. Asahi, T. Morikawa, T. Ohwaki, K. Aoki, Y. Taga, Visible light photocatalysis in nitrogen-doped titanium oxide, Science 293 (2001) 269–271.
[28] A. Gendanken, Using sonochemistry for the fabrication of nanomaterials, Ultrason. Sonochem. 11 (2004) 47–55.
[29] S. Lee, I.-S. Cho, D.K. Lee, D.W. Kim, T.H. Noh, C.H. Kwak, S. Park, K.S. Hong, J.-K. Lee, H.S. Jung, Influence of nitrogen chemical state on photocatalytic activities of nitrogen-doped TiO_2 nanoparticles under visible light, J. Photochem. Photobiol. A 213 (2010) 129–135.
[30] S. Livraghi, A.M. Czoska, M.C. Paganini, E. Guamello, Preparation and spectroscopic characterization of visible light sensitized N doped TiO_2 (rutile), J. Solid State Chem. 182 (2009) 160–164.
[31] S. Higashimoto, M. Azuma, Photo-induced charging effect and electron transfer to the redox species on nitrogen-doped TiO_2 under visible light irradiation, Appl. Catal. B 89 (2009) 557–562.
[32] Z. Chen, G. Zhao, H. Li, G. Han, Effects of water amount and pH on the crystal behavior of a TiO_2 nanocrystalline derivate from a sol-gel process at a low temperature, J. Am. Ceram. Soc. 92 (5) (2009) 1024–1029.
[33] I. Siti Aida, S. Srimala, Effect of pH on TiO_2 nanoparticles via sol–gel method, in: Proceedings of ICXRI 2010 International Conference on X-rays & Related Techniques in Research & Industry June 9–10 (2010), pp. 84–87.
[34] I. Siti Aida, S. Srimala, Effect of pH on TiO_2 nanoparticles via sol–gel method, Adv. Mater. Res. 173 (2011) 184–189.
[35] K. Prasad, D.V. Pinjari, A.B. Pandit, S.T. Mhaske, Phase transformation of nanostructured titanium dioxide from anatase-to-rutile via combined ultrasound sol–gel technique, Ultrason. Sonochem. 17 (2010) 409–415.
[36] C. Cantau, T. Pigot, J.-C. Dupin, S. Lacombe, N-doped TiO_2 by low temperature synthesis: stability, photo-reactivity and single oxygen formation in the visible range, J. Photochem. Photobiol. A 216 (2010) 201–208.
[37] B. Liu, L. Wen, X. Zhao, The structural and photocatalytic studies of N-doped TiO_2 films prepared by radio frequency reactive magnetron sputtering, Sol. Energy Mater. Sol. Cells 92 (2008) 1–10.
[38] H. Slimen, A. Houas, J.-P. Nogier, Elaboration of stable anatase TiO_2 through active carbon addition with high photocatalytic activity under visible light, J. Photochem. Photobiol. A 221 (2011) 13–21.
[39] J. Senthilnathan, L. Philip, Photodegradation of methyl parathion and dichlorvos from drinking water with N-doped TiO_2 under solar radiation, Chem. Eng. J. 172 (2–3) (2011) 678–688.